

# A RPC test station based on ROOT and VME

Zhi-Peng Lü<sup>1</sup> · Qing-Min Zhang<sup>1</sup> · Jie Zhao<sup>2,3</sup> · Jia-Wen Zhang<sup>2,3</sup> ·  
Yu-Guang Xie<sup>2,3</sup> · Sen Qian<sup>2,3</sup> · Zhe Ning<sup>2,3</sup> · Jeremiah Monari Kebwaro<sup>1</sup> ·  
Yu-Chi Chen<sup>1</sup> · Zi-Xing He<sup>1</sup>

Received: 24 June 2015 / Revised: 23 July 2015 / Accepted: 1 August 2015 / Published online: 14 April 2016

© Shanghai Institute of Applied Physics, Chinese Academy of Sciences, Chinese Nuclear Society, Science Press China and Springer Science+Business Media Singapore 2016

**Abstract** Due to its advantages in large-area application situations, the R&D of the resistive plate chamber (RPC) has always been carried out. A performance test station for RPC R&D has been designed and developed based on the VME bus and ROOT in Linux. This system can be customized expediently according to the requirements of different tests, which facilitates detector R&D because of its automatic HV scan, especially for long-term test. With this system, we have implemented the RPC performance test, including the efficiency curve, counting rate, dark current and charge and timing resolution.

**Keywords** Resistive plate chamber · VME · ROOT · R&D · Test station

## 1 Introduction

Because of its simple structure, high efficiency, and low cost, the resistive plate chamber (RPC) has been employed in many high-energy physics and astrophysics experiments, such as BaBar [1], Belle [2], OPERA [3], BESIII [4], the Daya Bay experiment [5, 6], and those at LHC [7–9]. At

the same time, a number of studies on improvements made in the RPC are also being constantly implemented since its invention in the early 1980s [10]. There is no doubt that the performance test is an inevitable process for RPC R&D, including the front-end electronics study [11, 12], and the long-term aging study [13]. Therefore, we have developed a test station to meet the research requirements for RPC. The test station based on ROOT and VME has the following advantages. The software for the VME interface, data collection, and graphic display was based on the CERN ROOT software development platform [14] and written in C++ language. Due to these merits, when we carry out different testing experiments, we need not make a lot of changes to the software system or spend a lot of time debugging the program. Besides, compared to the test system developed in the Windows environment, the testing system operated in Linux has a lower dependence on the system and a greater stability [15]. We adopted the most popular VME system for the hardware. Compared to CAMAC, the VME bus is faster, which means a higher data transmission rate. The study of the VME in detector electronics for some experiments, such as the reactor neutrino experiment at Daya Bay, has been implemented successfully [16]. In addition, as an important part of the test station, the high-voltage control system has gotten a great promotion. The SY1527 power supply system, which represents CAEN's latest proposal for a high-voltage and low-voltage power supply [17], has substituted the SY127 that we used before [18]. The high-voltage control system can be controlled automatically by the program, which not only maintains the integrity of the experiment but also avoids intervention and relieves the burden on the experimenters. In short, this automated operating mode reduces human intervention and accelerates experimental progress.

---

✉ Qing-Min Zhang  
zhangqingmin@mail.xjtu.edu.cn

<sup>1</sup> Department of Nuclear Science and Technology, School of Energy and Power Engineering, Xi'an Jiaotong University, Xi'an 710049, China

<sup>2</sup> State Key Laboratory of Particle Detection and Electronics, Beijing 100049, China

<sup>3</sup> Institute of High Energy Physics, Chinese Academy of Sciences, Beijing 100049, China

In the test station, we used the VME crate, the QDC plug-in, the scaler, and the TDC plug-in to set up a small data acquisition system. With this system, we carried out the preliminary test of the RPC and have achieved the corresponding satisfactory results. In the next step of the research, we plan to implement some experiments, including the study of non-Freon gas mixtures for the RPC detector and the influence of different humidities on the RPC performance.

## 2 The hardware structure and function of the system

A block diagram of test station's hardware is shown in Fig. 1, which is comprised of the gas control system, the high-voltage supply system, the trigger system, the signal processing system, the diagnosis system, and the data acquisition system.

The functions of these systems are described below. (1) The gas control system aims to supply working gas for the gaseous detectors and monitor gas flow, which is essential in the gas circulation process in terms of mass flow rate measurement. By using the gas control system, we can get information about gas mixtures for RPCs [19]. (2) The high-voltage supply system provides the detectors with the working electric voltage that they need, which plays an important role in the R&D of the RPC. The SY1527 power supply system can communicate with the computer via the RS232\_COM interface or the TCP/IP protocol [20]. The supplier provides dynamic-link libraries [17] (CAENHV Wrapper) based on Linux/Windows for users. The users can realize the automatic control of the high-voltage system by calling the dynamic-link libraries. (3) In the test station, the trigger system that is comprised of three scintillators aims to select effective pure muon events for

triggering. Besides, in order to reduce the influences of noise accidental coincidence ( $R_n$ ) [21], three scintillators are used to generate a threefold coincidence of the signals in the cosmic-ray muon test experiment. (4) The signal processing system consists of the Model N844 discriminator and the Model N405 coincidence unit [22]. The Model N844 discriminator accepts original negative pulse signals generated by the detector and the telescope system and then produces corresponding NIM outputs. These NIM signals via the Model N405 coincidence unit are further processed and then input into the data acquisition system. In addition, the rate of accidental coincidence of noise can be reduced through the logic "AND" to supply much purer muon events for triggering. (5) The diagnosis system, such as the oscilloscope, is aimed at monitoring the output signal from every aspect and judges whether the output graph is normal or not. (6) The data acquisition system, including the VME crate, scaler, QDC plug-in, and TDC plug-in, is responsible for collecting data and intuitively presents the performance of the detector for the experimenters. The scaler is used to test the efficiency and counting rate, and the dark current is obtained from HV monitoring. As for the QDC and the TDC plug-in, they, respectively, correspond to the testing of charge and timing information. In a nutshell, these systems work together to make up a complete testing platform although all of them have respective functions.

The entire system is controlled by a PC operated in the Linux system. The connection of PC and data acquisition hardware is realized by the Model V2718, a 1-unit wide 6U VME master module, communicating with the PC via optical fiber cables. The working principle of the test system can be described as follows. When the trigger logic produces a starting signal to TDC or a gated signal to QDC, the TDC model or the QDC model will start the process of digital conversion and then stop the conversion when a stop signal to TDC or at a rear edge of the gated signal, and finally, a marking signal indicating completion of data collection will be generated for reading. The counting rate and the efficiency can be tested by using the PC to achieve the count of the scaler unit within the given time. In addition, the data will be stored in a text file. At the same time, if necessary, the graphs displayed on the PC monitor in real time can be copied to the specified file. When the data acquisition is accomplished at a fixed point, the HV system will automatically ramp up or down to the next test point. The DAQ interface is shown in Fig. 2.

The performance of the RPC is very sensitive to the running environment, such as temperature and humidity. Now, a weather station is used to record environmental variables with time, and then the environmental data can be imported into the analysis for further study of the RPC performance's dependence on weather.

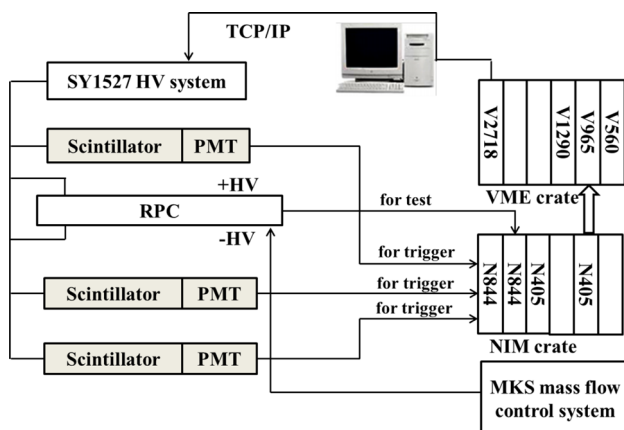


**Fig. 1** Connection of hardware of the test station

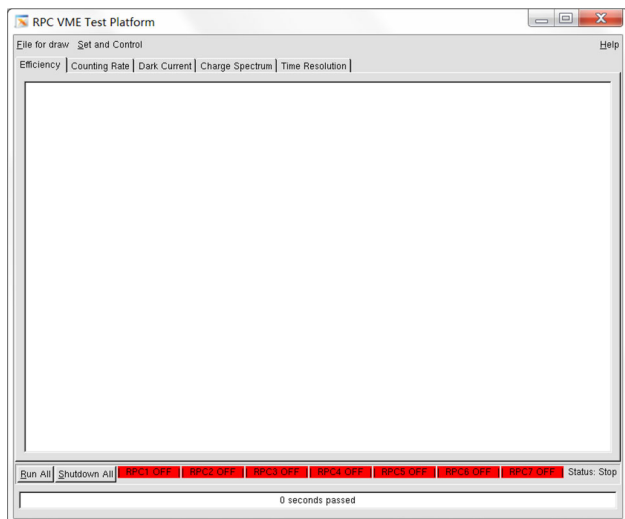


Fig. 2 DAQ interface

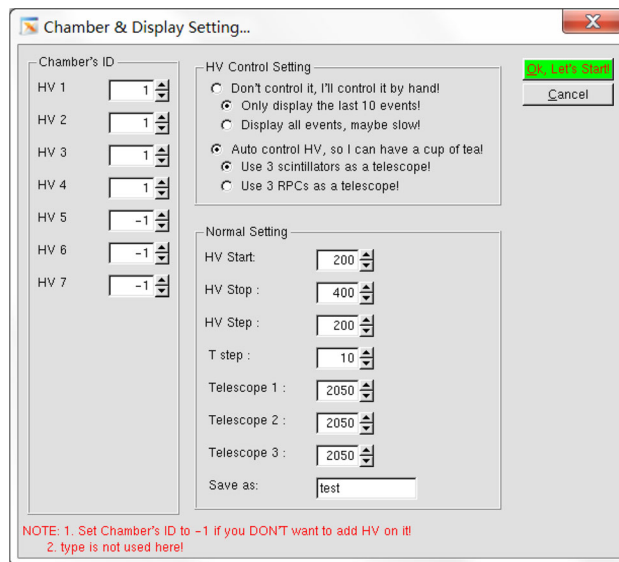


Fig. 3 High-voltage control interface

### 3 The software structure and function of the system

Flexibility and availability are the main factors to consider when choosing which programming language to use to develop a software system. C++, as an object-oriented programming language, can easily realize these features. In terms of the program structure, every plug-in stands for an object; therefore, we only need to transform or add an object to the program frame when we change or add a VME hardware device. The advantages of the program structure are summarized here. (1) The readability of the program is improved greatly due to the resemblance between software structure and hardware structure. (2) And it reduces the burden on programmers. The programmers can write the corresponding program with relative ease and need not use too much vigor to debug the program, as long as they know the hardware configuration. In the program, each object has the functions for initializing, prohibiting, reading data from and writing data into the corresponding module. When these objects are established, the program has been initialized the devices. So far, the programmers have developed the base class of the VME plug-in and some general plug-in classes. In the program system, the base classes of VME plug-ins follow the method of virtual function. Based on these reasons, for some special plug-ins, they can become new special classes, as long as they inherit the base classes and simply the special parts. As shown in Fig. 3, we have realized the automatic control of high-voltage through the software system. In short, this kind of software structure has brought great convenience to testing work.

### 3.1 The test of counting rate and efficiency

To confirm the feasibility of the test system, we conducted a cosmic-ray test experiment in which a special type of oil-free Bakelite resistive plate chambers developed by the IHEP was used [23]. The special type of oil-free resistive plate is produced by lamination at a high pressure with its outmost layers pre-immersed into melamine-formaldehyde resin, which guarantees an excellent surface quality [24, 25]. The Model V560 scaler, a 1-unit wide VME module providing 16 independent 32-bit counting channels [26], is used to complete the testing of the counting rate and efficiency. The testing principle of efficiency is described in Fig. 4, a threefold coincidence of the signals from the three scintillators as the input of the number 0 channel, and a fourfold coincidence of the signals from the RPC and three scintillators as the input of the number 8 channel. The inputs of the number 8 channel in unit time stand for the counting rate of RPC within the given time. The efficiency of the RPC is determined by the

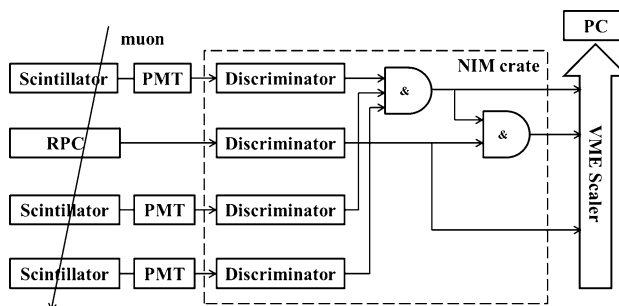
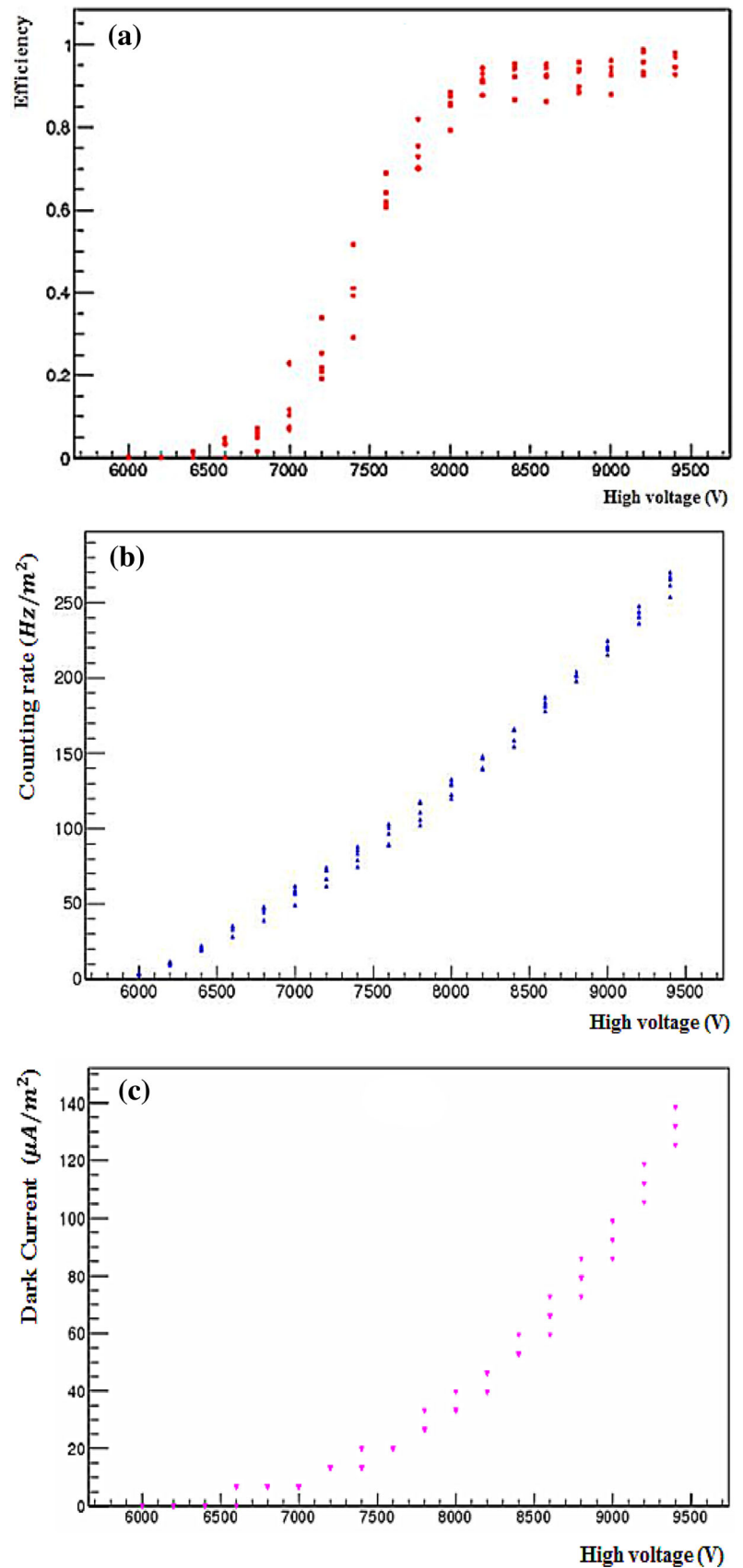
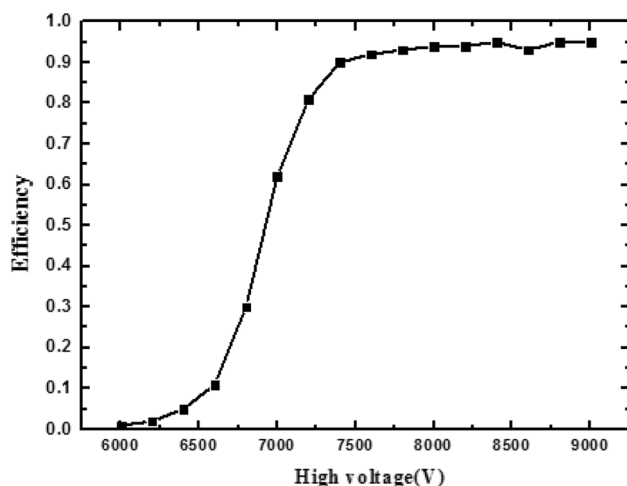


Fig. 4 Schematic diagram for the testing of counting and efficiency

**Fig. 5** Efficiency (a), counting rate (b), and dark current (c) versus high voltage





**Fig. 6** Curve of the average efficiency

ratio between the number of fourfold coincidences and the number of threefold scintillator triggers [27].

Before testing the counting rate and efficiency, we must first initialize the program to set up the device object, which includes the high-voltage module, the scaler module, and the ADC module. We can set the experiment parameters in the control interface to meet the requirements of the experiment. As shown in Fig. 3, the start and end values of the voltage are adjusted, along with the voltage step. Based on the voltage step, each testing point corresponds to a fixed value and the test time of each point has also been set. When everything is ready, we can click the start button in the control interface. When the voltage controlled by the program is up to an assigned value, the data acquisition system begins to get the data information. After completing the counting, the scaler is terminated by the program and will wait for the voltage scanning to the next working point. In order to reduce the experimental error to a reasonable range, a large amount of data requiring a long test time need to be collected. Based on these reasons, each experimental point should be measured several times to guarantee the reliability of data and to maintain the system's stability. During the experiment, the experimenters can easily observe the count of each channel of scaler and the efficiency of the detectors versus the high voltage by using the diagram and data in real time. After the experiment, all the testing data and figures are stored in the named files, which are convenient to be analyzed further. When the temperature of our laboratory is set at  $20 \pm 2$  °C and the gas mixture used is Ar:C<sub>2</sub>H<sub>2</sub>F<sub>4</sub>:iso-C<sub>4</sub>H<sub>10</sub> = 53:43:4, the test results of the performance of the RPC in streamer mode for a few loops are displayed online, as shown in Fig. 5. The three graphs, from top to bottom, represent the curve of efficiency, the counting rate, and the dark current, respectively. This test station system can run

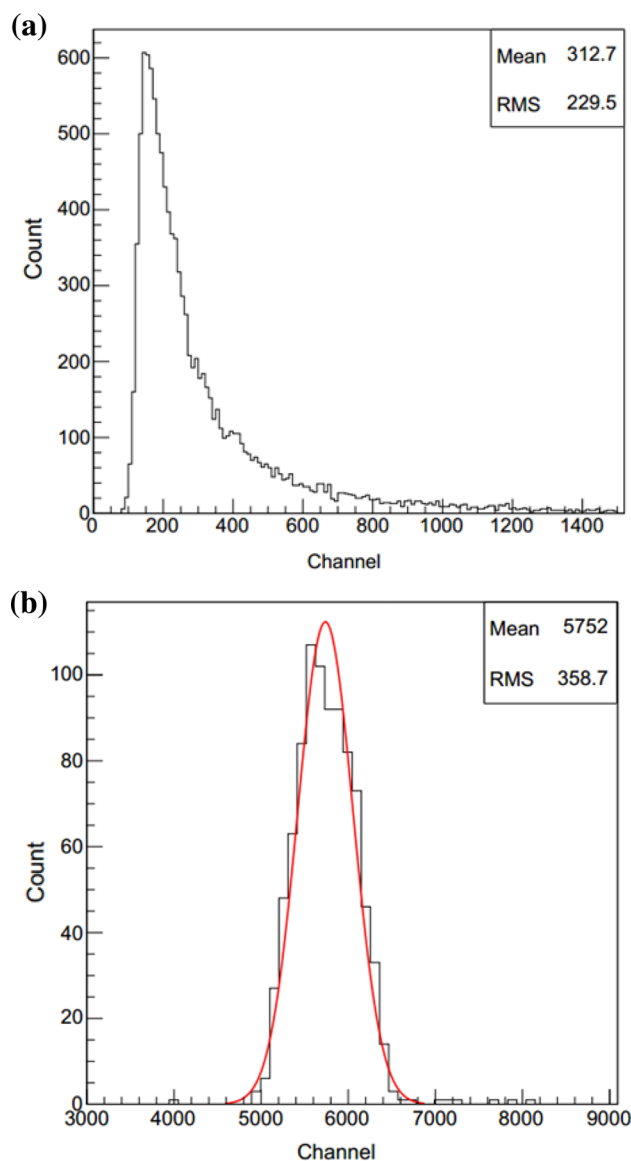


**Fig. 7** Test of signal charge (a) and time resolution (b)

periodically with the present HV range and HV step, so the different data points at a given HV are from different run loops.

Besides, it is convenient for us to analyze data offline. Figure 6 is obtained by combining the data from a few continuous test loops. If necessary, the experimenters can automatically run loop by loop continuously, maintaining continuity in the experiments.

### 3.2 The test of signal charge and time resolution

The testing of the signal charge and time resolution is also important functions of the test system. We used VME Model V965A QDC and V1290N TDC to realize the goals. The Model V965A is a 1-unit wide VME 6U module

housing 8 charge-to-digital conversion channels and one GATE input common to all channels. The principle of operation is described as below [28]. When the GATE input signal is active, the integrated currents received from the channel inputs are converted into voltage levels by the QAC sections. Each input signal is converted into two parts: one featuring 100pC full scale and the other 900pC full scale. They will only be stored in the data memory when the values are above a specified threshold and overflow doesn't occur in the memory. The Model V1290N is a 1-unit wide VME 6U module that houses 16 independent multi-hit event time-to-digital conversion channels [29]. When the trigger logic produces a starting signal to TDC, the TDC model will start the process of digital conversion until receiving a stop signal from the RPC. The timing information of the signal measured via data processing is presented in real time. We have used the telescope system and the detector to simulate the testing of the signal charge and time resolution. The testing process is similar to the efficiency mentioned above. It is also necessary to initialize the program to set up the device object. The only difference was that the high voltage was fixed in a certain value. The testing results in streamer mode are shown in Fig. 7. In this figure, the X-axis stands for the channel number with 200 fC/channel and 25 ps/channel, respectively. The signal amplitude can be up to a few hundred mV when the resistive plate chambers work in the streamer mode. Because of the noise and the fluctuation of measured signals, the charge spectrum and the timing resolution spectrum have a statistical fluctuation. Because of extremely pure cosmic-ray triggers during the test, the pedestals are also mostly invisible in the two plots of Fig. 7 and the offset of channel 5752 is from the fixed difference between the start signal and stop signal. Accordingly, the average charge is about 62.5 pC and the timing resolution (RMS) is approximately 9.0 ns. In this paper, we used the RPC detector to test the function of the test station, so we did not do the calibration of the ADC counts and the correction of time the resolution. But if necessary, a known amplitude signal can be tested to do the calibration.

## 4 Conclusion

We have successfully designed and developed a ROOT and VME RPC based test station that can be used on a Linux platform. The system can meet the automation measurement requirements of the general detector and will play an important role in further R&D of the Bakelite resistive plate chamber. We used the software system to test the performance of the RPC in different conditions and got meaningful results. In short, due to its automation measurement, long testing time, and good continuity, the

test station not only provides great control over statistical error and experimental error, but also will save a lot of manpower and experimental time.

**Acknowledgments** This work was supported by the National Natural Science Foundation of China (No. 11305124) and the Fundamental Research Funds for the Central Universities (No. xjj2013082).

## References

1. B. Aubert, A. Bazan, A. Boucham et al., The BABAR detector. Nucl. Instrum. Methods Phys. Res., Sect. A **479**, 1–116 (2002). doi:[10.1016/S0168-9002\(01\)02012-5](https://doi.org/10.1016/S0168-9002(01)02012-5)
2. A. Abashian, K. Gotow, N. Morgan et al., The belle detector. Nucl. Instrum. Methods Phys. Res., Sect. A **479**, 117–232 (2002)
3. S. Dusini, D. Autiero, E. Borsato et al., Design and prototype tests of the RPC system for the OPERA spectrometers. Nucl. Instrum. Methods Phys. Res., Sect. A **508**, 175–180 (2003). doi:[10.1016/S0168-9002\(03\)01346-9](https://doi.org/10.1016/S0168-9002(03)01346-9)
4. Y. Xie, J. Zhang, J. Chen et al., First results of the RPC commissioning at BESIII. Nucl. Instrum. Methods Phys. Res., Sect. A **599**, 20–27 (2009). doi:[10.1016/j.nima.2008.10.013](https://doi.org/10.1016/j.nima.2008.10.013)
5. Daya Bay Collaboration, 2007. arXiv: hep-ex/0701029
6. Z. Ning, Q. Zhang, J. Xu, et al. Calibration algorithms of RPC detectors at Daya Bay Neutrino Experiment. 2013 JINST 8 T03007 doi:[10.1088/1748-0221/8/03/T03007](https://doi.org/10.1088/1748-0221/8/03/T03007)
7. ALICE Collaboration, TDR of the Muon spectrometer, CERN/LHCC 99-22, 13 August 1999
8. ATLAS Collaboration, ATLAS Muon technical design report, CERN/LHCC 97-22, 5 June 1997
9. C.M.S. Collaboration, Muon project. CERN/LHCC **97–32**, 15 (1997)
10. R. Santonico, R. Cardarelli, Development of resistive plate counters. Nucl. Instrum. Methods Phys. Res. **187**, 377–380 (1981). doi:[10.1016/0029-554X\(81\)90363-3](https://doi.org/10.1016/0029-554X(81)90363-3)
11. F. Dou, H. Liang, L. Zhou et al., A precise time measurement evaluation board for a radiography system of high-Z materials. Nucl. Sci. Tech. **23**, 284–288 (2012). doi:[10.13538/j.1001-8042/nst.23.284-288](https://doi.org/10.13538/j.1001-8042/nst.23.284-288)
12. J.B. Xi, H. Liang, S.T. Xiang et al., Upgrade to the front-end electronics of the BESIII muon identification system. Nucl. Sci. Tech. **25**, 020402 (2014). doi:[10.13538/j.1001-8042/nst.25.020402](https://doi.org/10.13538/j.1001-8042/nst.25.020402)
13. C. Lu, RPC electrode material study. Nucl. Instrum. Methods Phys. Res., Sect. A **602**, 761–765 (2009). doi:[10.1016/j.nima.2008.12.225](https://doi.org/10.1016/j.nima.2008.12.225)
14. A. Yamaguchi, in *Fourth International Workshop on Resistive Plate Chambers and related Detectors*, Naples, Italy, 1997, p. 281
15. J.W. Zhang, J.F. Han, Q. Liu et al., The general detector test system under Linux based on Root interface. Nucl. Electron. Detect. Technol. **25**, 590–593 (2005). (in Chinese)
16. H.F. Hao, H. Liang, L. Zheng et al., Development of VME system in RPC electronics for reactor neutrino experiment at Daya Bay Nuclear Power Plant. Nucl. Sci. Tech. **24**, 010401 (2013). doi:[10.13538/j.1001-8042/nst.2013.01.002](https://doi.org/10.13538/j.1001-8042/nst.2013.01.002)
17. <http://www.caen.it/jsp/Template2/CaenProd.jsp?parent=20&idmod=122>
18. J. Zhang, Z. Du, J. Han et al., A new surface treatment for the prototype RPCs of the BESIII spectrometer. Nucl. Instrum. Methods Phys. Res., Sect. A **540**, 102–112 (2005). doi:[10.1016/j.nima.2004.10.037](https://doi.org/10.1016/j.nima.2004.10.037)
19. L. Ma, Y. Wang, J. Zhang et al., Study of RPC gas composition using Daya Bay RPCs. Chin. Phys. C **34**, 1116–1121 (2010)

20. S. Qian, Y.F. Wang, J.W. Zhang et al., A test system based on LabVIEW for RPC-Gd thermal neutron detector. *Nucl. Electron. Detect. Technol.* **28**, 883–888 (2008). (in Chinese)
21. Q. Zhang, Y. Wang, J. Zhang et al., An underground cosmic-ray detector made of RPC. *Nucl. Instrum. Methods Phys. Res., Sect. A* **583**, 278–284 (2007). doi:10.1016/j.nima.2007.09.052
22. <http://www.caen.it/csite/CaenProd.jsp?parent=12&idmod=114>
23. Q. Zhang, Z. Lv, J. Zhang, et al. Development of oil-free Bakelite resistive plate chambers for particle experiments. 2014 JINST 9 C07020. doi:10.1088/1748-0221/9/07/C07020
24. J.W. Zhang, H.Q. Zhao, R.B. Li et al., Research and development of large area resistive plate chamber. *HEP&NP* **27**, 615–618 (2003). (in Chinese)
25. J. Zhang, R.B. Li, Z.Z. Du et al., Study of different gas mixtures for RPC detector. *HEP&NP* **27**, 1019–1022 (2003). (in Chinese)
26. <http://www.caen.it/csite/CaenProd.jsp?parent=11&idmod=62>
27. J. Zhang, S. Qian, J. Chen et al., The BESIII muon identification system. *Nucl. Instrum. Methods Phys. Res., Sect. A* **614**, 196–205 (2010). doi:10.1016/j.nima.2009.12.036
28. <http://www.caen.it/csite/CaenProd.jsp?parent=11&idmod=454>
29. <http://www.caen.it/csite/CaenProd.jsp?parent=11&idmod=796>